China Steel Technical Report, No. 38, pp.60－65, (2025)

Development of Cu-Ga and Cu-Ga-Alkali Metal Fluoride Sputtering Targets for CIGS Solar Cells

RONG-ZHI CHEN

New Materials Research & Development Department
China Steel Corporation

This study presents the development of Cu–30 at.% Ga and Cu-30 at.% Ga–alkali metal fluoride (NaF/KF) sputtering targets for use in copper indium gallium selenium (CIGS) thin-film solar cells. To overcome the brittleness of cast Cu-30 at.% Ga, a powder metallurgy approach using pre-alloyed Cu–Ga powders with various Ga contents was employed. The resulting targets exhibited enhanced bending strength and reduced brittleness due to the formation of the less brittle ζ-phase (Cu_3Ga). Furthermore, a two-step wet mixing method was developed to uniformly incorporate NaF or KF into the targets, yielding dense composite structures with well-dispersed alkali metal fluorides. These targets were subsequently used to fabricate CIGS absorber layers via co-sputtering, followed by selenization and sulfurization. The co-doping of sodium and potassium significantly enhanced the photovoltaic performance, with the best-performing devices achieving a power conversion efficiency of 15.19%. The proposed fabrication methods not only improve target reliability but also contribute to the advancement of high-efficiency CIGS solar cells.

Keywords: Copper indium gallium selenium, Solar cell, Sputtering target, Powder metallurgy

1. INTRODUCTION

Due to the depletion of petroleum resources and the worsening problem of global warming, supporting green energy development has become an important responsibility for the CSC Group. In recent years, the development of materials for the solar cell industry has been one of the main research topics in CSC's R&D division. This includes the development of sputtering targets for copper indium gallium selenium (CIGS) solar cells. The basic structure of a CIGS solar cell is shown in Figure 1 [(1)]. From bottom to top, it includes a substrate (glass, metal foil, or polyimide), a back electrode (Mo), an absorber layer (CIGS), a buffer layer (CdS), an upper electrode layer (i-ZnO), and a transparent conductive layer (ZnO:Al or ITO). The absorber layer is usually made by vacuum sputtering.

In recent years, many studies have shown that adding potassium, an alkali metal similar to sodium, to the CIGS absorber layer can improve the efficiency of CIGS solar cells[(2-8)]. The common method is co-evaporation. In this process, NaF is first placed on the CIGS surface, and then KF is added, as shown in Figure 2[(5)]. *Wüerz et al*. found that potassium works in a similar way to sodium.

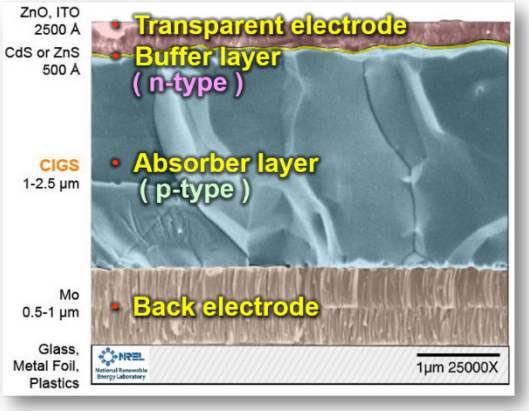

Fig.1. Schematic diagram of the structure of a CIGS solar cell[(1)].

Both can reduce the interdiffusion of indium and gallium. This helps to form a V-shaped gallium distribution, which improves the collection of p-type carriers. When both sodium and potassium are doped into cells on flexible steel substrates, the efficiency can reach 17.3% [(2)].

2. EXPERIMENTAL METHOD

This study focuses on the development of Cu–30at.% Ga and Cu–30at.% Ga–alkali metal fluoride sputtering targets. As shown in Figure 3, Cu–Ga pre-alloyed powders (Cu–15, 25, 30, and 35 at.% Ga) were first prepared via argon gas atomization. Cu–15 and Cu–25 at.% Ga powders were then mixed with Cu–35 at.% Ga powder in specific ratios to produce Cu–30 at.% Ga composition, which was sintered and densified by hot pressing. To fabricate Cu–30 at.% Ga–alkali metal fluoride targets, powder metallurgy was used. Given the low NaF/KF content (~2 vol.%), a two-step wet-mixing process was adopted. A small portion of Cu–Ga alloy powder was first mixed with NaF or KF using alcohol as a solvent, followed by uniform mixing with the remaining Cu–Ga powder. The resulting mixture was dried, sieved, and hot-pressed to obtain dense composite targets.

CIGS solar cells were fabricated by DC-magnetron sputtering of Mo back contacts onto glass substrates, followed by co-sputtering of precursor films using Cu–30 at.% Ga and Na-doped Cu–30 at.% Ga targets (developed by CSC) along with an In target. The films were selenized at 550°C in a Se-containing graphite box under Ar, and subsequently sulfurized at 550°C in an Ar/H_2S atmosphere, forming Cu(In,Ga)$(Se,S)_2$:Na absorbers. A CdS buffer layer was deposited by CBD, followed by ZnO/AZO transparent conductive layers via sputtering. Finally, the Al top electrodes were deposited by e-beam evaporation. The active area was 0.4 cm^2. Device performance was evaluated via J–V measurements under standard conditions (AM1.5, 100 mW/cm^2, 25°C) using a calibrated solar simulator.

3. RESULTS AND DISCUSSION

3.1 Fabrication of Cu–30 at.% Ga and Cu-30 at.% Ga-Alkali Metal Fluoride Targets

Cu–30 at.% Ga is the primary target composition adopted by CIGS solar cell manufacturers. However, according to the Cu-Ga binary phase diagram (Figure 4) [9], bulk Cu–30 at.% Ga ingots fabricated by traditional casting are very brittle. This brittleness is because of the formation of large amounts of the γ-phase (Cu_9–Ga_4), a brittle intermetallic compound that forms during solidification. As a result, it is hard to obtain a uniform, fine microstructure through later thermomechanical processing.

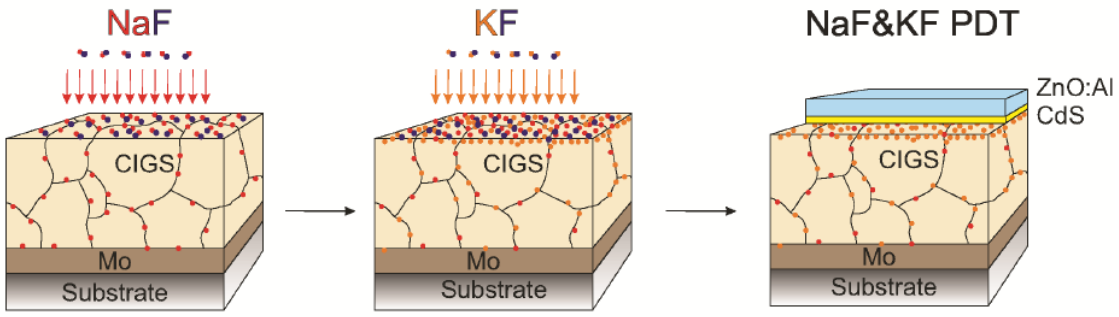

Fig.2. Schematic illustration of the post-deposition treatment (PDT) process using NaF and KF via evaporation[5].

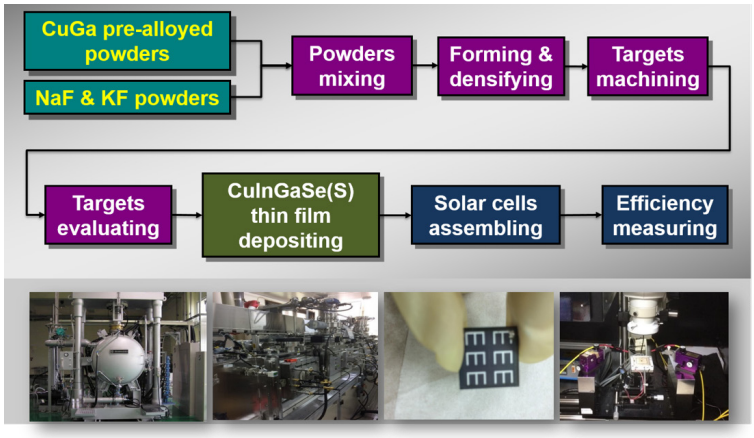

Fig.3. Experimental flowchart of this study.

In this study, Cu–30 at.% Ga targets were made by powder metallurgy with different powder mixing methods. Table 1 shows the relative density and three-point bending strength of the sintered targets. The results show that using a mixture of Cu–Ga pre-alloyed powders with varying Ga contents improves bending strength compared with using only Cu-30 at.% Ga powder. In particular, incorporating more Cu–Ga powders with less than 30 at.% Ga further enhances the mechanical strength of the targets.

The optical micrographs of the cross-sectional microstructures of Cu-30 at.% Ga targets prepared by different mixing methods are shown in Figure 5. No significant difference in grain size was observed, indicating that the variation in bending strength is not related to grain size.

X-ray diffraction (XRD) patterns of the Cu–30 at.% Ga targets prepared by different mixing methods are shown in Figure 6. The results confirm that the main phase in all samples is the γ-phase (Cu_9–Ga_4). However,

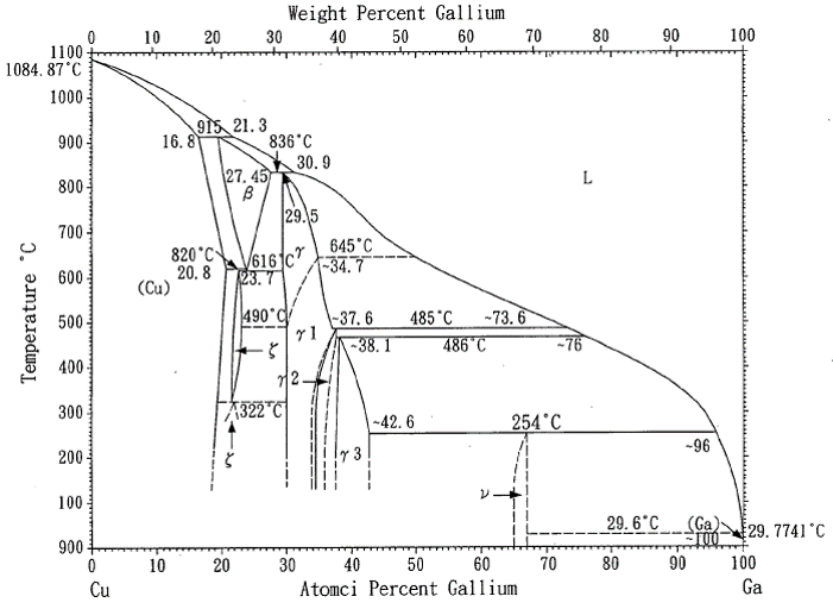

Fig.4. Cu–Ga binary phase diagram[9].

Table 1 Relative density and bending strength of Cu–30 at.% Ga targets prepared by different mixing methods.

Cu-30at.%Ga target	Relative density (%)	Bending strength (MPa)
CG30-A	100	216.3 ± 5.9
CG30-B	100	225.9 ± 7.9
CG30-C	100	418.1 ± 8.4

PS. CG30-A: 100% Cu-30at.%Ga power
CG30-B: Cu-35at.%Ga Power: Cu-15at.%Ga power = 75.5 : 24.5 (wt.%)
CG30-C: Cu-35at.%Ga Power: Cu-25at.%Ga power = 50 : 50 (wt.%)

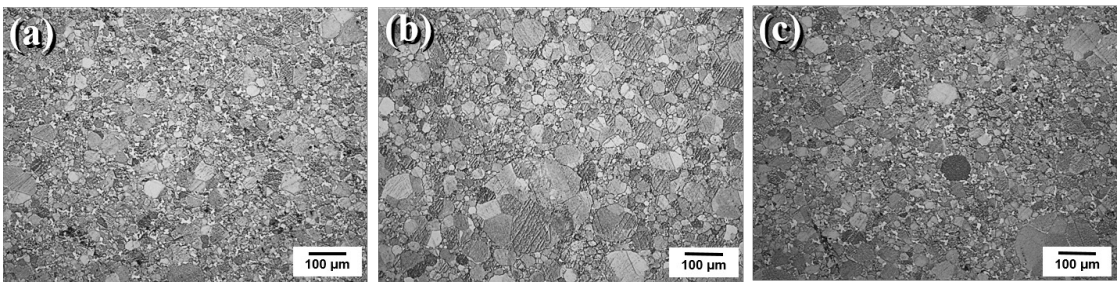

Fig.5. Optical micrographs of (a) CG30-A, (b) CG30-B, and (c) CG30-C targets.

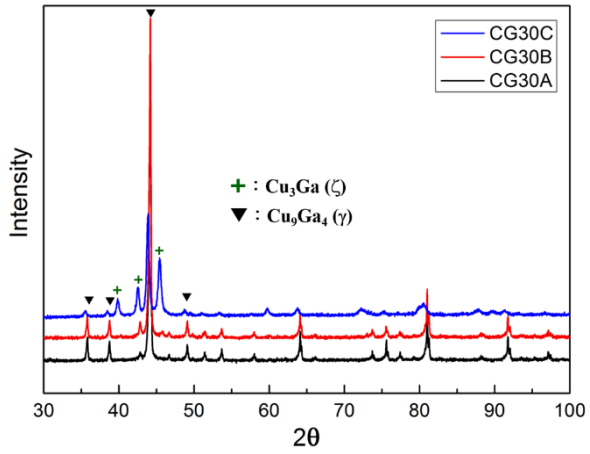

Fig.6. Phase identification by XRD analysis of the Cu–30 at.% Ga targets with different mixing processes.

when more Cu–Ga powders with lower Ga content were used, more of the ζ-phase (Cu_3–Ga), which is less brittle, appeared. This phase transformation improved the bending strength and reduced the brittleness of the targets, thereby reducing the risk of cracking during subsequent precision machining.

The cross-sectional optical micrographs of Cu–Ga-NaF targets prepared by different processing methods are shown in Figure 7. The dark regions correspond to NaF, with an estimated volume fraction of approximately 2%. The images correspond to: (a) two-step wet mixing, (b) one-step wet mixing, (c) dry mixing, and (d) a commercial target. In the two-step wet mixing process, a small portion of Cu–Ga alloy powder was first mixed with all of the NaF powder in an ethanol solvent, followed by the addition of the remaining Cu–Ga powder for further mixing. In contrast, the one-step method involves mixing all Cu–Ga and NaF powders simultaneously with ethanol. While the dry mixing process was conducted without any solvent. All subsequent hot-pressing parameters were identical to those used in the two-step wet mixing process. As shown in Figure 7, the two-step wet mixing method produces a uniform microstructure with well-dispersed NaF, superior to that of the commercial target.

Figure 8 shows the cross-sectional optical micrographs of Cu–30 at.% Ga–NaF and Cu–30 at.% Ga–KF targets. The volume fraction of the alkali metal fluorides is approximately 2%. It was clearly observed that the Cu–Ga-alkali metal fluoride targets fabricated using the two-step wet mixing process exhibited fine microstructures and a highly uniform distribution of the alkali metal fluorides.

Additionally, this work has been granted two invention patents in the ROC (Patent No. I551704 and Patent No. I573882).

3.2 Efficiency Analysis of CIGS Solar Cell Devices

Figure 9 shows the external quantum efficiency (EQE) curves of CIGS absorber layers deposited using

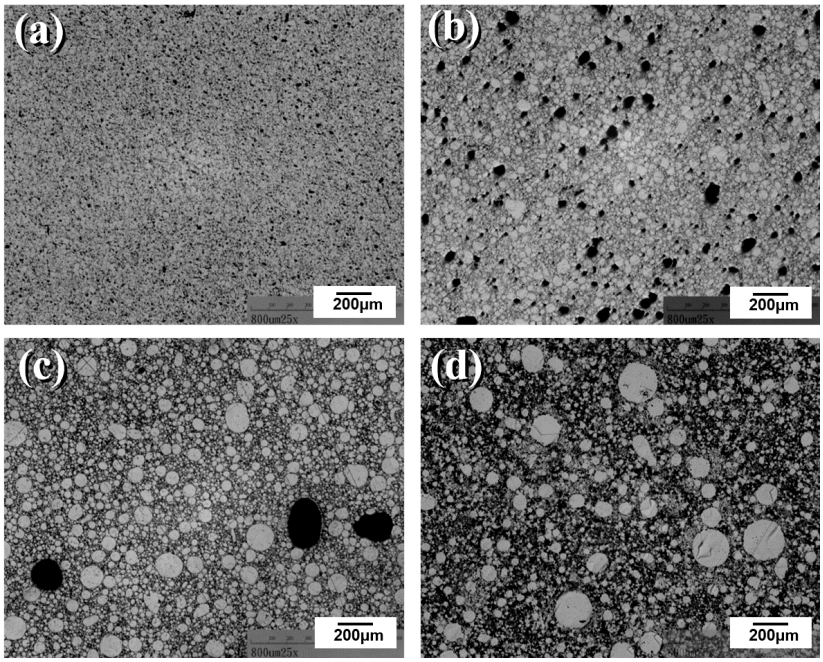

Fig.7. Optical micrographs of Cu–Ga–NaF target cross-sections prepared by different methods: (a) two-step wet mixing, (b) one-step wet mixing, (c) dry mixing, and (d) commercial target. The dark areas indicate NaF.

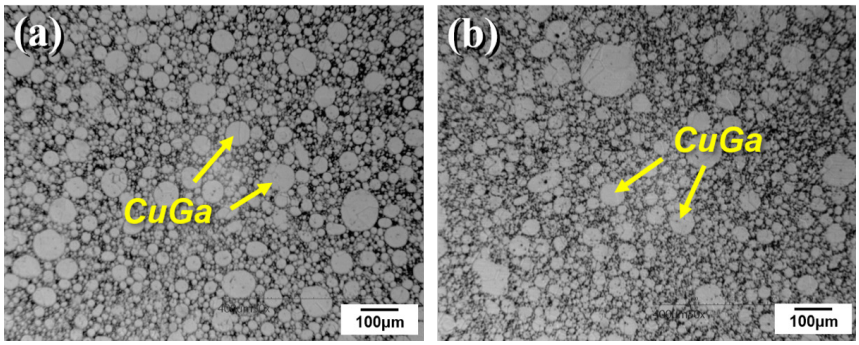

Fig.8. Microstructures of (a) Cu–30 at.% Ga–NaF and (b) Cu–30 at.% Ga–KF targets.

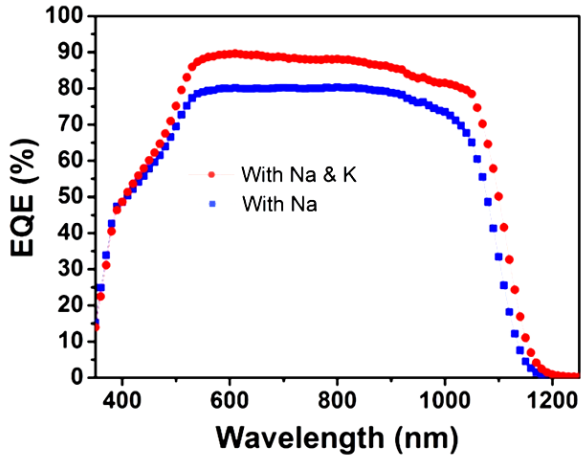

Fig.9. EQE spectrum of the CIGS devices doped with Na/K and devices doped with Na-only.

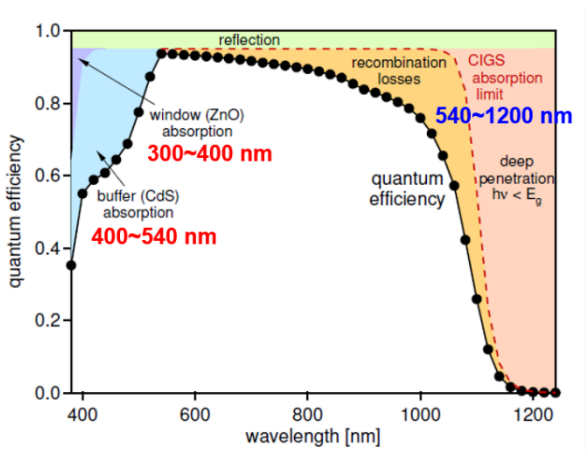

Fig.10. Schematic diagram showing the influence of each layer in a CIGS solar cell on quantum efficiency[10].

CSC-fabricated targets and subjected to selenization and sulfurization treatments. EQE refers to the ratio of the number of charge carriers (electrons or holes) collected by the solar cell to the number of incident photons at a given wavelength. It measures how effectively the device converts incoming light into usable electrical current. According to the literature[9], each layer of the solar cell affects the quantum efficiency only at specific wavelength ranges. By analyzing the quantum efficiency in different wavelength regions, the quality of each layer can be evaluated. As shown in Figure 10[10], the quantum efficiency between 300 nm and 400 nm corresponds to the window layer (ZnO), the range from 400 nm to 540 nm corresponds to the buffer layer (CdS), and the quantum efficiency from 540 nm to 1200 nm represents the CIGS absorber layer. The curves in Figure 9 clearly show that the EQE of the cell co-doped with Na and K (red curve) is significantly higher than that of the cell doped with Na only (blue curve).

The current–voltage (J–V) characteristics of CIGS–Na/K and CIGS–Na solar cells are shown in Figure 11. Both the solar cells co-doped with Na and K and those

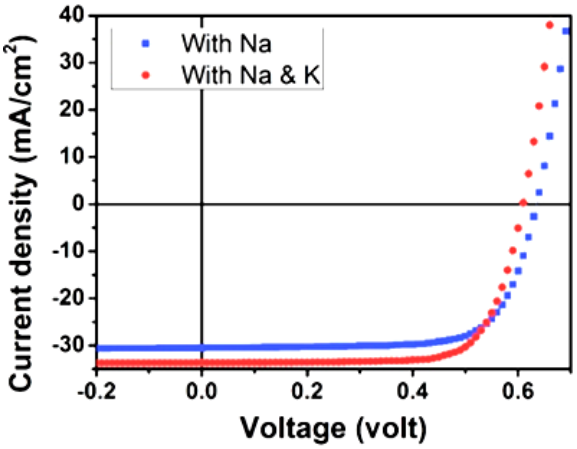

Fig.11. J–V curves of CIGS–Na/K and CIGS–Na devices.

doped with Na only exhibit well-rectangular J–V curves. The corresponding electrical parameters of both devices are summarized in Table 2. The data indicate that the Na/K co-doped cells exhibit higher fill factors and short-circuit current densities than the Na-only doped cells.

Table 2 P hotovoltaic parameters of the CIGS–Na/K and CIGS–Na devices.

	V_{oc} (mV)	J_{sc} (mA/cm^2)	FF (%)	η (%)
CIGS-Na	635	30.43	72.5	14.01
CIGS-Na/k	610	33.68	74.0	15.19

Consequently, the power conversion efficiency of the Na/K co-doped cells reaches 15.19%.

4. CONCLUSIONS

In this study, Cu–30 at.% Ga sputtering targets were successfully fabricated using powder metallurgy techniques with various powder mixing strategies. The results revealed that mixing Cu–Ga pre-alloy powders with different gallium contents, particularly those containing less than 30 at.% Ga, significantly enhanced the bending strength and reduced the brittleness of the sintered targets. X-ray diffraction analysis confirmed that this improvement is primarily due to the increased formation of the less brittle ζ-phase (Cu_3–Ga) in samples with lower Ga content. Furthermore, Cu–Ga-alkali metal fluoride targets produced through a developed two-step wet mixing process exhibited refined microstructures and a uniform distribution of alkali metal fluorides. This innovative process has been granted two invention patents in the ROC (Patent Nos. I551704 and I573882), recognizing its technical contribution.

The fabricated targets were then used to deposit CIGS absorber layers via sputtering, followed by selenization and sulfurization. External quantum efficiency (EQE) measurements showed that solar cells co-doped with sodium (Na) and potassium (K) exhibited higher efficiency in the 540-1200 nm wavelength range compared to cells doped with Na only. In addition, current-voltage (J–V) measurements demonstrated that Na/K co-doped cells achieved improved fill factors and short-circuit current densities, resulting in a power conversion efficiency of 15.19%.

Overall, this work not only enhances the mechanical performance of Cu–Ga targets through optimized powder mixing methods but also provides a reliable approach for incorporating alkali metal fluorides, ultimately contributing to improved photovoltaic performance of CIGS solar cells.

REFERENCES

1. Noufi, R. CIGS PV Technology: Challenges, Opportunities, and Potential. *NCPV, NREL*, 2013.
2. Wüerz, R., *et al*. CIGS Thin-Film Solar Cells and Modules on Enameled Steel Substrates. *Solar Energy Materials and Solar Cells*, 2012, Vol. 100, pp. 132-137.
3. Chirilă, A., *et al*. Potassium-Induced Surface Modification of Cu(In,Ga)Se_2 Thin Films for High-Efficiency Solar Cells. *Nature Materials*, 2013, Vol. 12, pp. 1107-1111.
4. Reinhard, P., *et al*. Features of KF and NaF Post-Deposition Treatments of Cu(In,Ga)Se_2 Absorbers for High-Efficiency Thin Film Solar Cells. *Chemistry of Materials*, 2015, Vol. 27, pp. 5755-5764.
5. Pianezzi, F., *et al*. Unveiling the Effects of Post-Deposition Treatment with Different Alkaline Elements on the Electronic Properties of CIGS Thin Film Solar Cells. *Physical Chemistry Chemical Physics*, 2014, Vol. 16, pp. 8843-8851.
6. Jackson, P., *et al*. Compositional Investigation of Potassium-Doped Cu(In,Ga)Se_2 Solar Cells with Efficiencies up to 20.8%. *Physica Status Solidi (RRL) - Rapid Research Letters*, 2014, Vol. 8, pp. 219-222.
7. Friedlmeier, T. M., *et al*. Improved Photocurrent in Cu(In,Ga)Se_2 Solar Cells: From 20.8% to 21.7% Efficiency with CdS Buffer and 21.0% Cd-Free. *IEEE Journal of Photovoltaics*, 2015, Vol. 5, pp. 1487-1491.
8. Republic of China Invention Patent. Publication No.: TW201139702A1, 2011. (In Chinese)
9. Huang, W. C., *et al*. Copper-Gallium Alloy Sputtering Target, Method for Fabricating the Same, and Related Applications. *U.S. Patent No. US20100116341 A1*, 2010.
10. Gloeckler, M. Device Physics of Cu(In,Ga)Se_2 Thin-Film Solar Cells. Dissertation, Department of Physics, Colorado State University, 2005.